



Review

Deep Learning and Federated Learning for Screening COVID-19: A Review

M. Rubaiyat Hossain Mondal ¹, Subrato Bharati ^{1,2}, Prajoy Podder ¹ and Joarder Kamruzzaman ^{3,*}

¹ Institute of Information and Communication Technology (IICT), Bangladesh University of Engineering and Technology (BUET), Dhaka 1205, Bangladesh; rubaiyat97@iict.buet.ac.bd (M.R.H.M.); subratobharati1@gmail.com (S.B.); prajoykuet09@gmail.com (P.P.)

² Department of Electrical and Computer Engineering, Concordia University, Montreal, QC H3G 1M8, Canada

³ Centre for Smart Analytics, Federation University Australia, Ballarat, VIC 3842, Australia

* Correspondence: joarder.kamruzzaman@federation.edu.au

Abstract: Since December 2019, a novel coronavirus disease (COVID-19) has infected millions of individuals. This paper conducts a thorough study of the use of deep learning (DL) and federated learning (FL) approaches to COVID-19 screening. To begin, an evaluation of research articles published between 1 January 2020 and 28 June 2023 is presented, considering the preferred reporting items of systematic reviews and meta-analysis (PRISMA) guidelines. The review compares various datasets on medical imaging, including X-ray, computed tomography (CT) scans, and ultrasound images, in terms of the number of images, COVID-19 samples, and classes in the datasets. Following that, a description of existing DL algorithms applied to various datasets is offered. Additionally, a summary of recent work on FL for COVID-19 screening is provided. Efforts to improve the quality of FL models are comprehensively reviewed and objectively evaluated.

Keywords: coronavirus; computed tomography; COVID-19; deep learning; federated learning; DenseNet



Citation: Mondal, M.R.H.; Bharati, S.; Podder, P.; Kamruzzaman, J. Deep Learning and Federated Learning for Screening COVID-19: A Review. *BioMedInformatics* **2023**, *3*, 691–713. <https://doi.org/10.3390/biomedinformatics3030045>

Academic Editor: Alexandre G. De Brevern

Received: 25 July 2023

Revised: 15 August 2023

Accepted: 22 August 2023

Published: 1 September 2023



Copyright: © 2023 by the authors. Licensee MDPI, Basel, Switzerland. This article is an open access article distributed under the terms and conditions of the Creative Commons Attribution (CC BY) license (<https://creativecommons.org/licenses/by/4.0/>).

1. Introduction

The novel coronavirus disease (COVID-19) pandemic [1–3] began in December 2019, killing millions of people [4–8]. Table 1 compares different pandemics in terms of death cases. COVID-19 causes symptoms of fever, lung issues, dyspnea [9], etc. In severe cases, patients need admission to intensive care units [10]. In many countries, COVID-19 has created a massive burden on the healthcare system as the number of ICUs is limited. Maintaining social distancing and wearing facial masks were suggested by the World Health Organization (WHO). From late December 2020, vaccines were used for the mass people. Since January 2023, the occurrence of COVID-19 has been steadily decreasing, allowing most nations to resume their normal lives as they were before the pandemic. However, new variants of COVID-19 may emerge in the near future, against which we may not be fully protected by the existing vaccines. We will continue to face a public health threat as a result of the evolution of the virus, global dissemination, and persisting vulnerabilities within our communities. So, COVID-19 may remain a global health threat. Hence, predicting COVID-19 spread is still important for planning medical facilities and other issues.

Table 1. Comparison of fatalities of selected pandemics.

Pandemics	Number of Deaths
Spanish Flu	40–50 million
Third Plague	12 million
AIDS	25–35 million
COVID-19 (28 June 2023)	6.90 million

During the peak of the pandemic, there were long queues to conduct COVID-19 testing for patients. There was also a limited number of medical personnel and kits. Therefore, it is important to apply artificial intelligence (AI) to diagnose COVID-19 patients. There has been significant research interest in studying the data of COVID-19. Some of these studies only focus on data visualization [11–13], while others use data to predict the future trend of the infection and automatically diagnose the disease. Because of the rapid spread of this virus infection, it has been challenging to collect data in an organized way. In many cases, the collected datasets are not balanced and are not large enough to contain bias errors. Hence, a summary of these research works on data and algorithms will facilitate the ongoing studies on COVID-19.

Machine learning (ML) as well as deep learning (DL) [10,14–19] algorithms, that are the subsets of AI, are applied to different COVID-19 data samples. These works are reported in a number of research papers. The transmission dynamics and the prevention method of the virus are reported in one study [15,20]. The use of AI in managing the effects of COVID-19 is also studied [21,22]. AI and its subsets, ML and DL, are used in different contexts in order to identify patterns in data. DL can find patterns in large datasets and can quickly improve automatically when new data samples are available. On the other hand, ML can be used to predict the number of infected cases and the number of death cases. This is useful for policy makers to plan for policies and strategies. ML can also be used to classify suspected COVID-19 patients. DL can be applied to the data-driven diagnosis of COVID-19 patients. Automated disease detection using CT or X-ray images prevents the virus from spreading from patients to medical staff. Some DL-based support schemes use customized networks, while others use pretrained transfer learning-based networks. Along with some allied fields such as the Internet of Things (IoT), computer vision, big data, and smartphones, AI can contribute to managing COVID-19 [14–17,23–26]. A number of ML algorithms, such as support vector machine (SVM), linear regression, logistic regression, and a number of DL algorithms, including convolutional neural networks (CNNs), are studied in the literature [27–29]. DL methods have gained much attention in the context of COVID-19 as these algorithms can deal with complex problems after learning from training samples. DL learns in-depth by considering multiple layers in a sequential manner [30,31]. DL has several stages: gathering and preparing data samples, extracting important features, performing classification, and finally evaluating the performance. Preparing the data includes several preprocessing tasks such as removing unwanted noise elements and resizing and augmenting the data/images. One form of DL is the transfer learning approach, where a pretrained model with its weight and bias values from one context is used in a similar but different context for retraining or testing. Deep transfer learning saves time as it enables quick convergence of the learning [32,33]. In the literature, several deep transfer learning models are reported; some of these are Visual Geometry Group (VGG), AlexNet, ResNet, Xception, Inception, MobileNet, densely connected convolutional networks (DenseNet), etc. [34]. One major issue in the use of data-driven diagnosis for COVID-19 is the challenge of ensuring patient privacy while exchanging information across healthcare providers. Using data gathered from many sources, federated learning (FL) creates a global DL model while still protecting the privacy of individual entities. In other words, FL can be used to train DL models in a distributed and private manner. It will be shown later in this paper that some recent works have discussed the potential of the FL approach in the context of COVID-19 diagnosis.

The literature review of this paper was performed using the preferred reporting items of systematic reviews and meta-analysis (PRISMA) guidelines [35]. Note that the PRISMA guidelines are essential for carrying out a rigorous and transparent literature review. They provide a structured framework for reporting and conducting systematic reviews and ensure reproducibility of systematic reviews. They contribute to the systematic review process, reduce bias, and improve reporting quality, and consequently, are popular in medical and healthcare research. We considered the papers from 1 January 2020 to 28 June 2023. Only English language papers were considered, and other language papers

were excluded. Two Boolean operators, “AND” and “OR” were used to identify necessary keywords. We searched several keywords; these were coronavirus, COVID-19, artificial intelligence, deep learning, transfer learning, federated learning, X-ray, ultrasound imaging and computed tomography. We ignored the clinical, epidemiological, and basic science aspects of COVID-19. We obtained a total of 11,700 papers on the application of DL and FL to COVID-19 from various publishers and preprints. The search criteria that resulted in 11,700 papers are shown below.

(“COVID-19”) OR (“coronavirus”)) AND ((“deep learning”) OR (“transfer learning”) OR (“federated learning”)) AND ((“computed tomography”) OR (“X-ray”) OR (“ultrasound imaging”)).

We manually excluded 11,260 articles from 11,700 articles as these were out of the main research interest of this paper. We reviewed the remaining 440 articles. Next, the most relevant 95 articles were cited in the paper and 72 were used for result synthesis. The selection of these 72 papers was made because these papers reported a description of COVID-19 datasets and performance results of the application of DL and FL to the diagnosis of COVID-19 patients. Figure 1 illustrates the summary of the PRISMA technique applied in this paper.

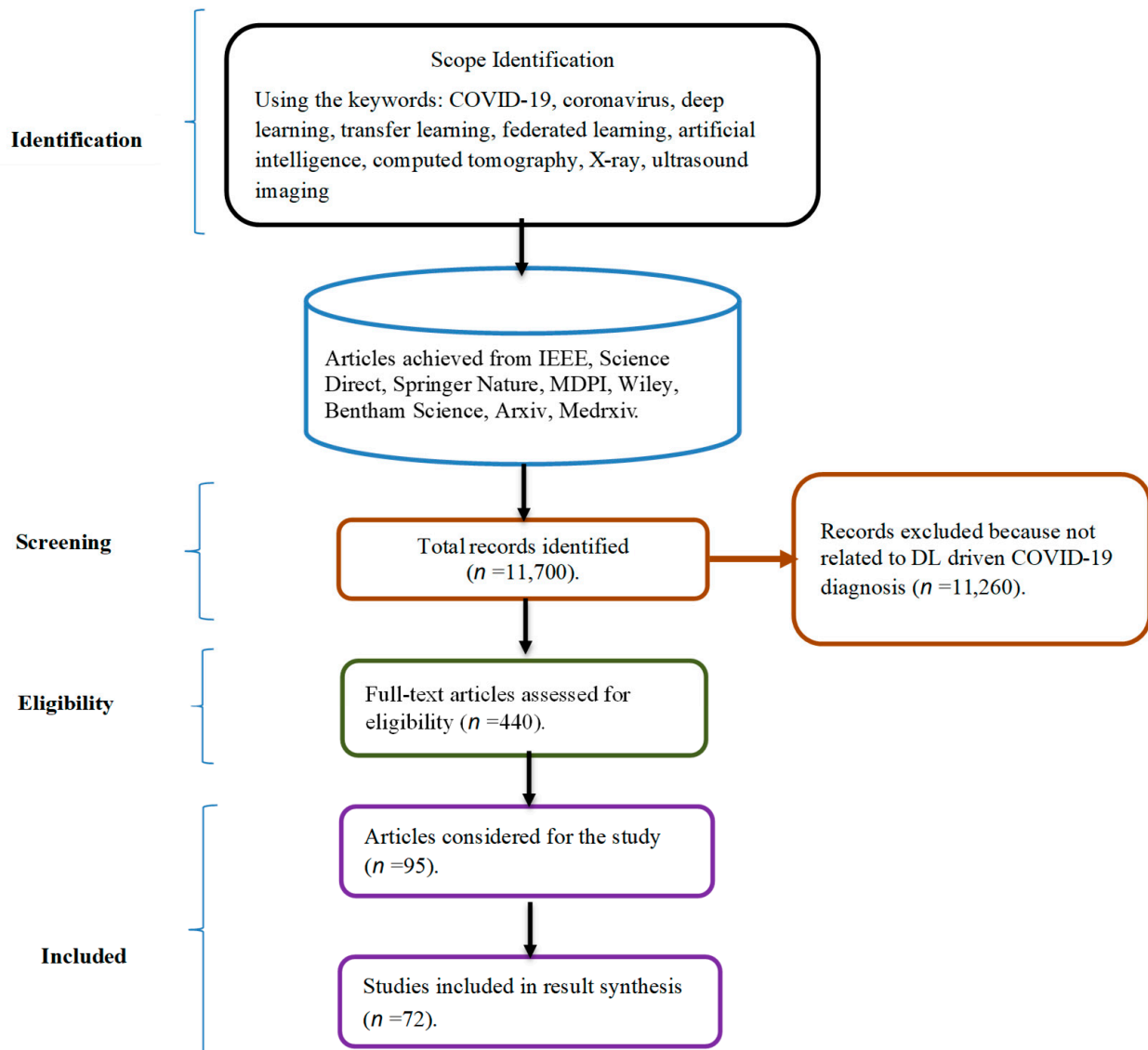


Figure 1. Literature survey using PRISMA guidelines.

The results of different algorithms are dependent on the datasets considered; hence, the performance of different DL algorithms reported in the literature needs a careful comparison. There are several survey or review papers [8,19–21,27–29,33,35] on COVID-19 that focus mainly on either ML/DL, or FL. Table 2 summarizes the aspects that these existing papers cover and how our work differentiates from other works and contributes to the survey on this topic. From Table 2, it can be seen that there is little work that reviews DL models and FL techniques simultaneously in the context of COVID-19 detection. Because of many recent studies in the application of DL and FL to combating COVID-19, there is a need for an up-to-date survey of the available datasets and algorithms applied to these datasets. This paper is motivated by the need to present a literature survey on the data-driven diagnosis of COVID-19 using DL models and FL techniques. The main contributions of this paper are as follows: A systematic detailed review is provided on different datasets of COVID-19, and DL algorithms that are applied to the datasets. Moreover, the application of FL when screening COVID-19 is also discussed. The review was performed for research articles published from 1 January 2020 to 28 June 2023 using PRISMA guidelines.

Table 2. Summary of some of the existing survey/review works on COVID-19.

Ref.	Year	Main Focus	Topics Not Covered
[8]	2022	Epidemiology, genomic sequence, and clinical characteristics of COVID-19	No details on the application of DL, does not focus on imaging datasets of COVID-19, no mention of FL
[19]	2021	Application of DL models to medical imaging and drug discovery for managing COVID-19	No mention of FL
[20]	2020	The epidemiology, clinical features, diagnosis, management, and prevention of COVID-19.	No details on the application of DL, does not focus on imaging datasets of COVID-19, no mention of FL
[21]	2020	ML, DL, and big data	No mention of FL
[27]	2020	Application of DL models, analyzing the impact of clinical and online data for COVID research	Does not focus on imaging datasets of COVID-19, no mention of FL
[28]	2020	Application of DL and edge computing	No details on the application of FL
[29]	2020	DL for image analysis and generating radiology reports	No details on the application of FL
[33]	2017	DL for medical image analysis	Not focusing on COVID-19 or pandemics
[35]	2021	ML and DL for COVID-19	No mention of FL
This work	2023	DL and FL for COVID-19 focusing on medical imaging, including X-ray, computed tomography (CT) scans, and ultrasound images	

The remaining sections of this work are structured as follows: Section 2 discusses the datasets that are widely used for COVID-19 detection. Section 3 discusses several metrics for performance. Section 4 describes the comparative performance of various DL algorithms in COVID-19 diagnosis. A survey is provided on FL for COVID-19 in Section 5. The paper discusses the new hybrid dataset in Section 6, and then the existing challenges and future work are described in Section 7. Finally, the paper provides concluding remarks in Section 8.

2. Datasets for DL

This section briefly describes different datasets available for the use of DL methods in COVID-19 diagnosis.

Table 3 shows some of the COVID-19 datasets that are reported in the literature [36–56]. In a dataset available on the Kaggle repository [36], there are 5863 chest X-ray images in .jpg format collected from Guangzhou Women and Children’s Medical Centre, Guangzhou. These images were collected from pediatric patients of ages ranging from one to five years. After quality control of the images, two experts graded the images. This dataset had three

folders for training, testing, and validation. Furthermore, the dataset had two subfolders, one for pneumonia and the other for normal cases [36]. Another dataset of 319 radiographic X-ray images created by the authors of [37] is available on GitHub [38]. These images were a collection of COVID-19, MERS, SARS, and ARDS, where 250 belonged to COVID-19-positive patients. A dataset termed as COVIDx containing 104,009 CT images of 1489 patients is available on GitHub [39]. Furthermore, a dataset called COVNet data containing 4563 CT images of 3506 patients from six medical centres is available on GitHub [40]. A dataset of pneumonia chest X-ray images is available in [57]. A dataset of 306 X-ray images is available in [42]. This dataset was organized in training and testing portions and categorized into patients marked as normal, bacterial pneumonia, COVID-19, and viral pneumonia. A dataset of 219 X-ray images of COVID-19 patients is available on the Kaggle repository [44]. In a study [58], a dataset of 295 chest images was generated by combining two individual datasets. This dataset is available in [43] and contains images of normal as well as 53 viral and bacterial pneumonia patients. Another dataset contains X-ray images of normal, COVID-19 patients, SARS patients, Streptococcus, and Acute Respiratory Distress Syndrome (ARDS) [45]. The research work in [59] presents Twitter datasets [46,53] containing tweet IDs on COVID-19. A database of SIRM COVID-19 [48] contains 94 chest X-ray and 290 lung CT scan images of 71 COVID-19 patients as of 10 May 2020.

Table 3. Available datasets on COVID-19.

Sl. No.	Name of the Dataset	Type of Dataset	References
1.	Chest X-ray images (pneumonia)	X-ray	[36]
2.	COVID-19-image data	X-ray	[37,38]
3.	COVIDx	CT	[39]
4.	COVNet	CT	[40]
5.	Google drive (Collected from Ref. [41])	X-ray	[42]
6.	Pneumonia sample X-ray	X-ray	[43]
7.	COVID-19 Radiography Database	X-ray	[44]
8.	CoronaHack:Chest X-Ray-Dataset	X-ray	[45]
9.	TWITTER COVID-19 CXR	X-ray	[46]
10.	COVID-19 Radiography Database	X-ray	[47]
11.	COVID-19 Database	X-ray	[48]
12.	Radiopedia	X-ray	[49]
13.	Chest Imaging	X-ray	[50]
14.	COVID-19 CT segmentation	CT	[51]
15.	COVID-19-CT-Seg-Benchmark	CT	[52]
16.	COVID-19-TweetIDs	Text (Social media)	[53]
17.	Coronacases Initiative	CT	[54]
18.	CO-IRv2	CT images	[55]
19.	X-ray images three levels	X-ray	[56]

A dataset comprises 32 chest X-ray images from Radiopedia [49]. A study presented 103 chest images of 50 cases in Spain [50]. In the Radiology Society of North America (RSNA) database, X-ray images of patients having traditional pneumonia and people without lung infection were available [60]. CT image samples of COVID-19 patients were reported in another study [61]. The dataset contained images of lungs and noted the type of infection. A research group in Norway created two datasets from more than 60 suspected patients; the two datasets had 100 and 829 CT scan slices [51]. The research work in [61] showed that DL is effective in detecting COVID-19 in CT scan images using

a dataset [52]. DL can be applied to heterogeneous datasets that include CT scan images of COVID-19 and non-COVID-19 [51]. Table 4 provides a comparison of different X-ray image datasets [62–74], while Table 5 compares the CT image datasets [75–89].

Table 4. Comparison of different X-ray datasets.

Datasets	Number of Images	No. of Positive Patients	Classes	Class Levels	Ref.
[36,37]	100	50	2	COVID-19, non-COVID-19	[62]
[39]	13,975	266	3	Normal, Pneumonia, COVID-19	[63]
[37,38]	5941	68	4	Bacterial Pneumonia, Normal, Viral Pneumonia (non-COVID-19), COVID-19	[64]
[37,38,42]	307	69	4	Pneumonia Virus Normal, Pneumonia Bacterial, and COVID-19	[41]
Collected from 6 institutes	213	106	2	COVID-19, Normal	[65]
[37,38]	127	125	3	COVID, Pneumonia, and No-Findings	[66]
[67] and Sylhet Medical College	6161	305	4	Viral Pneumonia (non-COVID), Bacterial Pneumonia, COVID-19, Normal	[68]
[37,38,69]	1256	284	4	Pneumonia Viral, Pneumonia Bacterial, COVID-19, Normal	[70]
[38,43,44]	458	295	3	Normal, COVID-19, and Pneumonia	[71]
Combination of [37,67]	5949	76	3	Normal, Pneumonia, and COVID-19	[72]
[36,38,48–50,73]	3487	423	3	Viral Pneumonia, Normal, COVID-19	[74]

Table 5. Comparison of different CT datasets.

Datasets	Number of Images	No. of Positive Patients	Classes	Class Levels	Ref.
Custom	499	-	2	COVID-19 positive and negative	[75]
Dataset from Renmin Hospital of Wuhan University	46,096	106 positive patients	2	51 patients having COVID-19 pneumonia, 55 control patients having any other diseases	[76]
Collected from 5 different hospitals in China	1136	723 positive cases	2	Positive cases and negative cases	[77]
Dataset reported in [40]	4356	3322	3	COVID-19, pneumonia, and non-pneumonic lung diseases	[78]
Sun Yat-Sen Memorial Hospital and Renmin Hospital of Wuhan University	275	88 positive patients	3	COVID-19, bacterial pneumonia, and healthy persons	[79]
Dataset reported in [80,81]	1020	108	2	COVID-19 positive and negative	[82]
[83,84]	2900	1232	2	COVID-19 and healthy images	[85]
[38,47,49,86]	1124	403	2	Non-COVID-19, COVID-19	[87]
Custom	150	-	3	Community acquired pneumonia, Non-pneumonia, COVID-19	[88]
The designated COVID-19 hospitals in Shandong Province	230	79	3	No pneumonia, common pneumonia, and COVID-19	[89]

Apart from the X-ray and CT images, there are datasets of other samples as well. Data from several medical imaging modalities can be combined to create multimodal imaging datasets for COVID-19 detection. Multimodal datasets combine the benefits of many imaging techniques and can provide a more comprehensive and accurate representation

of the disease. For instance, a multi-modal dataset can improve the model’s robustness to changes in data quality or missing information in a single modality of samples. In creating multimodal datasets, preprocessing the photographs to ensure they are in a consistent format, resolution, and orientation is a critical step. Table 6 briefly presents multimodal datasets [90,91] that were used for COVID-19 diagnosis. In addition, a dataset of ultrasound images is also shown. Table 7 shows a comparative summary of different preprocessing methods applied to different datasets of X-ray and CT scan images. The number of positive and negative samples in the dataset, and different data preprocessing techniques, for example, data segmentation, augmentation, rescaling, normalization, etc., are discussed. There are some clinical datasets, and there are also hybrid datasets created by the fusion of individual datasets. Classifications are performed into different classes: binary, tertiary, and quaternary. For example, studies [62,64,65,91–96] report datasets of X-ray images, while studies [97–99] focus on CT images. Some works [97,98] consider segmentation as data preprocessing, and perform binary classification of COVID-19 and non-COVID-19 cases. A recent work [99] performs data augmentation and normalization as preprocessing, and then computes a binary classification of COVID-19 cases and conventional lung disease cases.

Table 6. Comparison of different ultrasound and multimodal datasets.

Modalities	Datasets	Number of Diagnoses Images	No. of Positive Patients	Classes	Class Levels	Ref.
Ultrasound	Custom	58,924	35	3	COVID-19, suspected and symptomless	[90]
Multimodalities (Combination of X-ray and CT or others)	[37,38,69]	20 CT images and 117 chest X-ray images	137	1	COVID-19 pneumonia	[91]

Table 7. Comparative summary of the datasets and DL algorithms reported in the literature.

Reference	Modalities		Dataset	Number of Cases Used in Experiment	Data Preprocessing Techniques
	X-ray	CT			
[65]	✓	✗	Fusion of several datasets	COVID-19: 70 Pneumonia: 1008	Augmentation, Rescaling
[92]	✓	✗	Fusion of several datasets	COVID-19: 70 Pneumonia: 1008 SARS: 11	Augmentation, PCA, Feature Extraction by AlexNet architecture
[93]	✓	✗	Pneumonia (chest X-ray image) dataset	624 (Normal and Pneumonia)	Generative adversarial network
[100]	✗	✓	Clinical dataset	COVID-19: 219 Non-COVID-19: 399	Hounsfield Unit-based preprocessing
[101]	✓	✗	COVIDx	Bacterial Pneumonia: 931 Viral Pneumonia: 660 COVID-19: 45 Normal: 1203	Augmentation, Rescaling, Normalization
[62]	✓	✗	Fusion of several datasets	COVID-19: 50 Normal: 50	Rescaling
[102]	✗	✓	Clinical dataset	COVID-19: 368 Pneumonia: 127	Rescaling, Segmentation

Table 7. Cont.

Reference	Modalities		Dataset	Number of Cases Used in Experiment	Data Preprocessing Techniques
	X-ray	CT			
[64]	✓	✗	Fusion of several datasets	Bacterial Pneumonia: 2786 Viral Pneumonia: 1504 COVID-19: 68 Normal: 1583	Augmentation, Resizing
[82]	✗	✓	Clinical dataset	COVID-19: 108 Non-COVID-19: 86	-
[94]	✓	✗	Fusion of several datasets	COVID-19: 180 Normal: 8851 Pneumonia: 6054	-
[95]	✓	✓	Fusion of several datasets	COVID-19: 200 Normal: 200 Bacterial Pneumonia: 200 Viral Pneumonia: 200	-
[96]	✓	✗	COVIDx	COVID-19: 99 Non-COVID-19: 18,529	Augmentation
[103]	✗	✓	Clinical dataset	COVID-19: 3389 Non-COVID-19: 1593	VB-Net model for Segmentation and Lung Mask Generation
[104]	✓	✗	Fusion of several datasets	COVID-19: 158 Non-COVID-19: 158	-
[105]	✓	✓	Fusion of several datasets	COVID-19: 231 Normal: 1583 Bacterial Pneumonia: 2780 Viral Pneumonia: 1493	Augmentation, Normalization of Intensity, CLAHE Method
[106]	✓	✗	Fusion of several datasets	COVID-19: 135, Bacterial and Viral Pneumonia: 320	Augmentation
[107]	✗	✓	COVID-CT dataset	COVID-19: 345 Non-COVID-19: 397	Augmentation (GAN based), Resizing, Normalization
[108]	✓	✗	Fusion of several datasets	COVID-19: 180, Pneumonia: 6054, Normal: 8851	Augmentation
[109]	✓	✗	Kaggle datasets	COVID-19: 70, Normal: 80	Augmentation, Resizing
[91]	✓	✓	Fusion of several datasets	COVID-19: 117 (X-ray), 20 (CT), Normal: 117 (X-ray), 20 (CT)	Resizing, Data Normalization
[110]	✓	✗	Fusion of several datasets	COVID-19: 181, Normal: 364	Resizing, Data Normalization
[111]	✗	✓	Fusion of several datasets	COVID-19: 1684, Pneumonia: 1055, Normal: 914	Resizing
[112]	✓	✗	Fusion of several datasets	COVID-19: 142, Normal: 142	Augmentation, Resizing
[113]	✓	✗	Fusion of several datasets	COVID-19: 250, Other Pulmonary Diseases: 2753, Healthy Images: 3520	Augmentation, Resizing
[114]	✗	✓	UCSD-AI4H datasets	COVID-19: 349, Healthy Images: 397	Resizing, Data Normalization
[115]	✓	✗	Fusion of several datasets	COVID-19: 219, Normal: 1341, Viral Pneumonia: 1345	Augmentation, Resizing, Data Normalization
[116]	✓	✗	Fusion of several datasets	COVID-19: 536, Viral Pneumonia: 619, Normal: 668	CLAHE, Normalizing, White Balance Algorithm, Resizing

Table 7. Cont.

Reference	Modalities		Dataset	Number of Cases Used in Experiment	Data Preprocessing Techniques
	X-ray	CT			
[97]	✗	✓	Fusion of several datasets	COVID-19: 349, Non-COVID-19: 397	Segmentation, Augmentation
[98]	✗	✓	Data from ten hospitals	COVID-19: 656, Normal: 423	Segmentation and Classification
[99]	✗	✓	Fusion of two datasets	SARS-CoV-2: 1252, Other Lung Diseases: 1230	Data augmentation, Data Normalization
[55]	✓	✓	Fusion of two datasets	Normal: 1229 and COVID-19: 1252	Resizing, Data Normalization, Data Augmentation and Detection
[117]	✓	✗	Fusion of two datasets	Normal: 1583, Pneumonia: 4273, and COVID-19: 79	Resizing, Data Normalization, Data Augmentation and Detection
[118]	✓	✗	Data collected from 8 online sources	Healthy: 10,192, COVID-19: 3615	Fine-Tuning and Detection
[119]	✓	✗	Collected from various online sources	Normal: 4223, Pneumonia: 3674, and COVID-19: 2143	Segmentation and Detection
[120]	✗	✓	GitHub repository	COVID-19 positive: 1726 and negative cases: 1685	Resizing, Data Normalization, Data Augmentation and Detection

The majority of the datasets described above consist of CT or X-ray images, however, some are multimodal. The datasets include tertiary and quaternary classes in addition to binary data. The quality and diversity of the data, together with appropriate validation, are crucial components in creating trustworthy DL models for the datasets indicated above. These datasets are used by researchers to develop and improve DL algorithms that can diagnose COVID-19 effectively and accurately.

3. Performance Metrics Used for DL

Several performance metrics were considered while classifying and diagnosing COVID-19 [121–124]. These metrics depend on some true positive (TP), false positive (FP), true negative (TN), and false negative (FN) terms. Correctly detected positive patients are represented as TP. The term FP shows the negative or normal patients that are incorrectly recognized as positive. TN signifies that normal patients are correctly recognized as negative, while FN represents positive patients incorrectly recognized as normal patients. Classification accuracy indicates the correctness of classifying normal samples as normal and abnormal samples as abnormal.

The ratio of accurately classified COVID-19-positive patients to the total number of suspected patients is referred to as recall, and also known as sensitivity. The accuracy of predicting negative or normal cases is referred to as specificity. Precision, also known as positive predictive value (PPV), is the proportion of correctly identified positive instances to the total projected positive cases. The ratio of successfully identified negative samples to the total expected negative samples is the negative predictive value (NPV). The harmonic method of precision and recall is the F-measure. The area under the receiver operating characteristics curve (AUC) measures how accurately positive and negative instances are classified. The average of the absolute difference between the predictive and actual sample values is used to calculate the mean absolute error (MAE).

The performance metrics mentioned above offer a quantifiable technique to assess the efficacy of DL models when used to analyze imaging datasets in order to detect COVID-19. It is shown in the next section that these measures are used to assess the DL models and decide which one to deploy in practical situations.

4. Comparative Performance of Existing DL Algorithms

Recent research publications on AI for the management or detection of COVID-19 are available [125–165]. Some of these papers concentrate on FL approaches [133–145], some on survey work on DL [146–154], and yet others on original research works on DL [125–132,155–165].

Although many research papers have reported the use of DL for COVID-19, in the following, only the very recent studies [155–165] are described, while others are only summarized in Table 8. A framework for detecting COVID-19 from X-ray images consists of a modified version of DenseNet-121, an image data loader for batch separation, a loss function, and a weighted random sampler for balanced training [155]. The framework [155] achieves a decent diagnosis performance with an accuracy of 99.81%. Another study [156] creates an automated system for categorizing COVID-19 cases into two groups, while addressing concerns such as the limited and unbalanced dataset and model overfitting. The proposed VGG-16 based DL technique [156] obtains a remarkable 99.86% accuracy and 99.9% recall. One stacking ensemble model is created by combining the outputs of the multiple pretrained models, multi-layer perceptron (MLP), recurrent neural network (RNN), long short-term memory (LSTM), and gated recurrent unit (GRU) [157], in the case of two datasets of COVID-19 symptoms [157]. The COVID-CheXNet system [158] uses contrast-limited adaptive histogram equalization to improve the contrast of the X-ray images and Butterworth bandpass filters to decrease the noise level. Using the weighted sum rule at the score level, the COVID-CheXNet scheme correctly and accurately diagnoses COVID-19 patients with a detection accuracy rate of 99.99%, sensitivity of 99.98%, and specificity of 100% [158]. In one study [159], a CNN is employed to screen for COVID-19 using chest CT images and Resnet50, VGG16, VGG19, Densenet121, InceptionV3, and Xception. Comparing the VGG16 model against other models, it is found to be 98% correct for the cases considered [159]. The detection of COVID-19 and other pneumonia cases is proposed using a new DL-based model, COVIDWNet-GB [160] that is based on depth-wise dilated CNNs as well as feature reuse residual blocks. The proposed COVIDWNet-GB achieves a 96.81% accuracy in multi-class (COVID-19, Lung Opacity, Normal, and Viral Pneumonia) X-ray images [160]. An essential weights-only transfer learning method is reported for devices with low runtime resources [161] by reducing the model's less important weight parameters. The empirical results show that the pruned ResNet34 model can achieve 95.47% accuracy, 0.9216 sensitivity, 0.9567 F1-score, and 0.9942 specificity on the CT-scan dataset with 20.64% fewer weight parameters [161]. One study [162] considers DL models of ResNet50, ResNet101, DenseNet121, DenseNet169, and InceptionV3. These models are reported to perform satisfactorily, with ResNet101 outperforming the others, achieving 96% accuracy [162]. DL models VGG-19, ResNet-50, Inception v3, and Xception are optimized and compared after preprocessing the data [163]. The VGG-19 model, with fine-tuning, can detect COVID-19 with excellent accuracy—up to 94.17% for chest X-rays and 93% for CT scans [163]. A DL model termed SCovNet classifies COVID-19 when applied to 17,599 images with an accuracy of nearly 99% and 98% on chest CT images and X-ray images, respectively [164]. Explainable AI is gaining interest in the field of DL. According to one recent study on explainable AI, an encoder–decoder–encoder architecture-based DL framework is reported to provide a thorough, high-resolution, visual explanation of the classification outcomes for a dataset with four classes [165].

Table 8. Performance results of different DL algorithms.

Ref.	DNN Model	Accuracy (%)	Recall (%)	Precision (%)	F1-Score (%)	AUC (%)	Specificity (%)
[65]	ResNet 18	-	96	-	-	95.18	70.65
[92]	ResNet 18	95.12	97.97	-	-	-	91.87
[93]	ResNet 18	99	-	98.97	98.97	-	-
[127]	ResNet 18	86.7	81.5	80.8	81.1	-	-

Table 8. Cont.

Ref.	DNN Model	Accuracy (%)	Recall (%)	Precision (%)	F1-Score (%)	AUC (%)	Specificity (%)
[101]	ResNet 50	96.23	100	100	100	-	-
[65]	ResNet 50	98	96	-	-	-	100
[62]	ResNet 50	76	81.1	-	-	-	61.5
[64]	ResNet 50V2	-	-	-	-	-	-
[82]	ResNet 101	99.02	98.04	-	-	-	100
[94]	Xception and ResNet 50V2	99.56	-	-	-	-	-
[126]	ResNet 101	98.75	100	96.43	-	-	97.50
[96]	CoroNet	93.50	90	93.63	93.51	-	-
[103]	ResNet 34	87.5	86.9	-	82	94.4	90.1
[104]	ResNet 50	95.38	97.29	-	-	-	93.47
[105]	Inception ResNet V2	92.18	92.11	92.38	92.07	-	96.06
[106]	ResNet 50, VGG 16	91.24	-	-	-	94	--
[107]	ResNet 50	82.91	80.45	-	-	-	91.43
[108]	Xception and ResNet 50V2	91.4	-	-	-	-	-
[109]	VGG 16, VGG 19	97	100	-	-	-	94
[91]	DenseNet 121	99	-	96	96	-	-
[110]	VGG 19	96.3	-	-	-	-	-
[111]	Inception V1	95.78	-	-	-	99.4	-
[112]	VGG 16	97.62	97.62	-	-	-	78.57
[113]	VGG 16	97	87	-	-	-	94
[114]	DenseNet 121	90.61	90.8	89.76	90.13	-	-
[115]	DenseNet 201	99.4	-	99.5	99.4	-	-
[116]	COVID-Lite (2-level Classification)	99.58	99.58	100	99.79	99.34	100
[116]	COVID-Lite (3-level Classification)	96.43	96	97	96	99	97.89
[128]	Modified Inception	79.3	83	55	63	81	67
[98]	DCN	96.74	97.91	-	-	98.64	96.00
[99]	ResNet101	99.4	-	99.6	99.4	-	99.6
[125]	EDL-COVID	99.05	99.05	-	98.59	-	99.6
[129]	Mks-ELM-DNN	98.36	98.28	98.22	98.25	98.36	98.44
[130]	DenseNet201 + MLP	95.64	-	-	95.63	-	-
	MobileNet + SVM (Linear)	98.62	-	-	98.46%	-	-
[131]	CoroDet for 4 class Classification	91.2	91.9	92.04	90.04	-	93.48
[97]	CheXNet	87	-	-	86	75	-
[55]	CO-IRv2	96.18	97.23	95.35	96.28	95	95.08

Table 8. *Cont.*

Ref.	DNN Model	Accuracy (%)	Recall (%)	Precision (%)	F1-Score (%)	AUC (%)	Specificity (%)
[117]	CO-ResNet	90.90	-	90.20	-	-	-
[118]	Pretrained CNN	98.6	98.6	98.6	98.6	-	-
[119]	ResNet18 with Multiclass Classification Layers	96.43	93.68	-	93.0	-	99.0
[132]	VGG-19, BRISK, and RF	96.60	95.0	-	-	-	97.4
[120]	Optimized NASNet	82.42	78.16	-	-	91.00	-

Table 8 presents the comparative performance of different DL methods reported in the literature. The methods are compared in terms of a number of metrics: classification accuracy, sensitivity, precision, F1-score, AUC, and specificity. It can be seen that an excellent classification accuracy of 99.58% is obtained by the COVID-Lite algorithm. The recall value of COVID-Lite is also 99.58% [116]. The precision, F1-score, AUC, and specificity values of COVID-Lite are reported to be 100%, 99.79%, 99.34%, and 100%, respectively. The second-highest classification accuracy of 99.56% is reported for the Xception and ResNet 50V2 schemes [94]. In one study [125], the EDL-COVID algorithm is shown to have an accuracy of 99.05% with a recall value of 99.05%. The reported EDL-COVID scheme has an F1-score of 98.59% and a specificity of 99.60%. However, ResNet 50 [101], ResNet 101 [126], VGG 16, and VGG 19 [108] have recall values of 100%. Furthermore, ResNet 101 has an accuracy value of 98.75%, which is better than ResNet 50, VGG 16, and VGG 19. Among all the systems considered, the best AUC value of 99.40% is found for Inception V1 which has an accuracy of 95.78% [111]. On the other hand, the highest F1-score of 100% is achieved by ResNet 50 [101]. Hence, from Table 8, it can be seen that there is no single algorithm that has the best value for every metric.

As shown above, there are several stand-alone DL models and hybrid ones that are applied to different imaging datasets for COVID-19 detection. Researchers combine the concepts of individual DL algorithms and create new frameworks. Some of these hybrid architectures are called CoroNet, CoroDet, EDL-COVID, MKs-ELM-DNN, COVIDWNet-GB, etc., in the literature. The main DL models that are applied for the data-driven diagnosis of COVID-19 are illustrated in Figure 2.

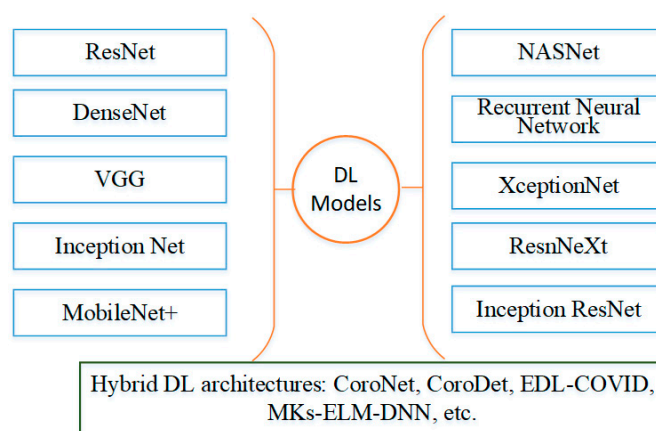


Figure 2. Illustration showing the DL models that are applied for COVID-19 diagnosis.

5. Survey on FL for COVID-19

This section explores the literature on the application of FL in the context of COVID-19. Existing studies [133–138] indicate that DL models can be trained using FL in a distributed,

private manner. This is crucial in situations where data collection and centralization are neither possible or desirable because of privacy concerns, transmission bandwidth restrictions, or legal restrictions. FL is used to safeguard organizations' data privacy by using less accurate local models to build a global DL model [133–138]. Clients train their own models locally, while the server employs an incentive mechanism and aggregates them until convergence occurs.

The FL frameworks described in [133] are reported to collect data, train an intelligent model, and then distribute this model throughout the public network in a decentralized fashion. By utilizing FL, hospitals are able to keep their patient data private and simply share weights and gradients, while the data are distributed around the facilities via blockchain [133]. The authors of [133] propose the use of blockchain to authenticate data and FL to train the model worldwide while still protecting the organization's confidentiality. In particular, COVID-19 patients are identified using a capsule network segmentation and classification algorithm [133] that deals with the heterogeneity of data first. The proposed federated capsule network is compared with DL models of VGG, ResNet, MobileNet, and DenseNet. The proposed federated blockchain-based capsule network achieves an accuracy value of 98.68% when applied to CT images [133].

Using FL for COVID-19 data training and deployment is suggested in another work [134]. Well-known DL models, MobileNet, ResNet, ResNeXt, and COVIDNet, are reported [134] to be tested with and without the FL framework to see which performed better. Training using the FL framework and training without the FL framework are compared in trials. ResNet performs well in training both with FL and without FL according to the results. With COVID-19 labels, ResNeXt performs the best. The smallest number of parameters can be found in MobileNet. As a result, the research shows that ResNeXt and ResNet are the best models for identifying COVID-19 for the datasets considered in the study [134]. Communication efficiency and model correctness are not considered in the works in [133,134]. Model performance cannot be guaranteed with FL's default option, which involves a high connection overhead for sending model updates. Medical diagnostic image analysis for COVID-19 detection is the subject of another research work [135], which presents a unique dynamic fusion-based FL approach with an emphasis on enhancing model performance and communication efficiency. An architecture for medical diagnostic image analysis based on dynamic fusion-based FL systems is first designed. According to their local model's performance, the participating clients are dynamically selected, and the model fusion is scheduled as per participating clients' training time. It has been determined that this strategy is viable and has superior model performance, communication efficiency, and fault tolerance compared with FL's default option [135].

The non-independent and identically distributed (non-IID) and imbalanced data distributions that naturally occur in the FL environment are investigated in one study [136]. The work [136] proposes VGG16 and ResNet50, two distinct FL model designs, and the studies show that the proposed models outperform centralized models. When applied to other medical imaging applications with massive, distributed, and privacy-sensitive data, it is possible that the FL approach in [136] could be more broadly applicable than the COVID-19 screening used in other studies. Using an FL technique to detect COVID-19-related CT anomalies in patients from a global study has been shown to be feasible [137]. Three Hong Kong hospitals were used as training and testing facilities, while four more independent datasets were sourced from mainland China or Germany to ensure model generalizability. Longitudinal scans of COVID-19 patients in the hospital are being used to test automated lesion burden estimation. In order to construct a privacy-preserving AI model for COVID-19 medical image diagnostics, FL algorithms are examined. In the study, a CNN-based DL model is taken into account for training the decentralized multicentre CT imaging data [137]. To deal with the unpredictability of the data and annotations, one paper [138] suggests a new federated semi-supervised learning technique. The performance disparity between training a model with one dataset and applying it to another is being studied using a multi-national database made up of 1704 scans from three different countries. A

total of 945 COVID-19 results are manually defined by radiologists. It is possible that semi-supervised learning can lessen the burden of annotations in a distributed situation by avoiding the requirement for sensitive data sharing. The suggested framework in [138] is shown to be more effective than a fully supervised scenario with traditional data sharing rather than model weight sharing [138]. FL has attracted the attention of researchers who work on topics such as training data clustering [139], multistage local training [140], and multitask learning [141]. Additionally, certain studies [142,143] are concerned with the design of incentive mechanisms to encourage clients to participate in FL tasks.

One study trains an FL model named electronic medical record chest X-ray AI model (EXAM) using data from 20 different institutions around the world utilizing vital signs, laboratory results, and X-rays from symptomatic COVID-19 patients [144]. Using data from all participating sites, EXAM is reported to achieve an AUC greater than 0.92 in terms of predicting outcomes 24 and 72 h after the patient first presented to the emergency room, and it improves the average AUC by 16% while increasing generalizability by 38% on average when compared to models trained using only data from a single site. At the largest independent test site, EXAM is shown to have a sensitivity of 0.950 and a specificity of 0.882 for predicting the need for mechanical ventilation or death within 24 h. The FL in [144] ensures faster data science collaboration and the creation of a model capable of predicting clinical outcomes in patients with COVID-19. Based on 231 major papers, one study [145] examines FL systems from a software engineering standpoint. The full lifetime of FL system development is covered in the data synthesis stage, which includes background understanding, requirement analysis, architectural design implementation, and assessment. It is reported that benchmarking approaches are necessary to evaluate FL system development in real-world COVID-19 situations with rich datasets and representative workloads [145]. In a recent study, an FL framework is introduced for the interpretation of medical diagnostic images to separate COVID-19 from four different chest illnesses [166]. The proposed FL framework in the DenseNet-169 DL model [166] successfully safeguards client privacy while accurately separating COVID-19 from four chest diseases with an accuracy of 98.45%. The main aspects and the main outcome of some of these prominent studies on FL-based COVID-19 detection are presented in Table 9.

Table 9. Summary of different FL methods for COVID-19 diagnosis.

Ref	Year	The Main Aspect of the Work	Findings
[133]	2021	Considering Blockchain to authenticate data, and capsule network for classification of CT images	The federated blockchain and capsule network achieves an accuracy value of 98.68%
[134]	2020	Evaluating MobileNet, ResNet, ResNeXt, and COVIDNet with and without FL	FL with ResNet and ResNeXt perform better than others
[135]	2021	Introducing a new dynamic fusion-based FL	The fusion-based FL approach achieves better model performance and communication efficiency
[136]	2021	Imbalanced data distributions that naturally occur in the FL environment are investigated	The proposed FL techniques with VGG16 and ResNet50 perform well
[137]	2021	CT images of three Hong Kong hospitals, and four in mainland China/Germany are used to ensure model generalizability.	FL with a CNN-based DL model works well
[138]	2021	A new federated semi-supervised learning technique is introduced and applied to 1704 samples of 3 countries.	The proposed method is more effective than a fully supervised scenario with traditional data sharing
[144]	2021	FL applied to X-ray images from 20 institutions	FL achieves an AUC of 0.92% which is better than DL models on single site
[166]	2023	FL with DenseNet-169 DL is investigated	The proposed FL with DenseNet-169 achieves an accuracy value of 98.45%.

The findings mentioned in the above papers would encourage researchers to use FL to build a powerful model for COVID-19 screening. While several works have applied FL to COVID-19, the field of FL application is still in its infancy, and numerous related challenges remain unresolved. Enhancing the quality of FL models is a current research focus and a difficult task.

6. Hybrid Dataset

In Section 2, several COVID-19 datasets are reviewed, where most of the datasets consist of either X-ray or CT scan images from a single source. In order to increase the number of samples in the dataset, samples of different datasets can be combined to form a hybrid dataset. There are several ways to form hybrid datasets, for instance, the formation of a new hybrid dataset is shown below.

The new hybrid dataset is formed by the fusion of two individual datasets found at [51,146]. One of the datasets [51] consists of 929 images where 473 are COVID-19-positive samples and 456 are of normal patients. In [51], image segmentation is already done, and the images and their associated masks are separately available. On the other hand, the other dataset [146] has 2482 images where 1252 are for COVID-19 patients and 1230 are for patients that are non-infected with the virus. The dataset in [146] has been collected from hospitals in Sao Paulo, Brazil, and these data samples do not have the masks separated. In order to combine the two datasets, the images of [146] are first segmented and then separated into the actual images and their masks. Next, the images and their associated masks for the two datasets are combined to form the hybrid dataset. There are a total of 3411 CT scans included in this dataset. There are 1726 CT scans that are positive for COVID-19. In contrast, there are 1685 normal CT scans, all of which test negative for SARS-CoV-2. The resultant dataset is available at [167].

In this research, the images are processed in two steps. In the first step, all the original images are examined, and the minimum dimensions of the images are found to be 224 by 224 pixels. After that, all the images are converted to the size of the minimum dimensions. Considering RGB images, the input dimension to CO-DenseNet is set as $224 \times 224 \times 3$. In the second step, the images are preprocessed according to the ImageNet dataset containing thousands of image classes and millions of image samples. The CO-DenseNet is trained using a pretrained network that is already trained on the ImageNet dataset. All the images are preprocessed by dividing each pixel intensity value by 255 followed by the ImageNet mean, and the result is divided by the standard deviation of ImageNet. After that, data augmentation is applied to increase the number of image samples and prevent the overfitting of the model. As part of augmentation, rotation, horizontal flipping, vertical flipping, and zoom range selection are performed where the zoom range is 0.2 which means zoom-in and zoom-out by 20%.

Given the scarcity of large COVID-19 datasets, hybrid datasets can aid in the generation of large samples and the appropriate evaluation of DL models.

7. Research Implications and Future Work

This section discusses the implications of this research work, existing challenges, and future scopes of work. This paper follows PRISMA guidelines to provide a systematic review of the application of DL methods in the data-driven diagnosis of COVID-19. PRISMA guidelines are followed in preparing this review. There are several review papers [150–154] in the literature that focus on DL-based COVID-19 management; however, this paper considers the latest research work on DL and FL, followed by the introduction of a proposed new DL method to manage COVID-19. Since the study and research outcomes of COVID-19 are changing rapidly, the findings of our review work need to be adjusted in the future. Issues related to the epidemiology, clinical aspects, treatment, and vaccine of COVID-19 are out of the scope of this review. The effectiveness of any classification algorithm varies depending on the dataset considered. Some datasets may have erroneous or incomplete labels that may lead to misleading results of the DL algorithm. Moreover, there is a lack of

benchmark datasets of COVID-19 patients. The algorithms should be applied to a number of large and correct datasets of COVID-19.

Many countries apply social distancing, lockdown, and similar approaches to mitigate the spread of the virus. There are also some challenges regarding the data privacy of the public. In the future, governments may create formal regulations when providing guidelines on applying social distancing and ensuring data privacy. AI, IoT, and wireless sensor networks can be used together to examine the presence of the virus in the environment. AI can be used to trace the spread of the virus, identify susceptible patients, and control the infection to some extent.

Moreover, AI can also predict the possibility of death cases based on the data of previous cases. DL methods can contribute to devising treatment plans and vaccines for COVID-19. DL can be used along with image processing techniques in recording the severity of chest and lung lesions and measuring the shape, length, and comparative changes in the lesions. The examination of the lesions may assist medical practitioners to make an efficient and quick decision regarding the stage of the disease. For effective data-driven diagnosis using DL, large and reliable datasets on COVID-19 should be formed from different hospitals. In order to provide a more thorough understanding of the disease, multimodal approaches and techniques should combine various modalities, such as various medical images (for example, X-rays and CT scans as multimodal datasets), clinical data (for example, symptoms, patient history), and laboratory tests (for example, PCR results). AI, along with other emerging technologies such as blockchain and the Internet of Drone Things [168], may be able to contribute to the management of pandemics.

In the future, there should be strong collaboration among experts in different disciplines such as medical, biological, image processing, and computer science. This collaboration will greatly help in devising new ways to fight against COVID-19.

8. Conclusions

This research examines the use of DL approaches in the fight against COVID-19. To begin, several X-ray, CT scans, and ultrasound image collections are described. The overall number of images, the number of positive COVID-19 samples, and the classes contained within the dataset are all listed in the description. Following that, a comparative description of several preprocessing methods applied to various datasets is presented, where the preprocessing techniques include data normalization, segmentation, rescaling, and augmentation. This review work also shows that DL approaches such as CNN, VGG-16, ResNet, VGG-19, COVIDNet, and hybrid neural networks may successfully diagnose COVID-19 when employed on X-ray and CT scan images. The review also covers the most recent advances in FL research and application, as well as a comparison of the effects of FL and non-FL products, with a particular emphasis on the use of FL in the diagnosis of COVID-19. In the future, studies should be carried out to collect high-quality X-ray and CT images for a significant number of suspected patients. To increase COVID-19 identification in a realistic scenario, new DL algorithms should be developed.

Author Contributions: M.R.H.M.—Conceptualization, Methodology, Writing—original draft, Writing—review and editing; S.B.—Methodology, Software, Visualization, Resources, Writing—review and editing; P.P.—Methodology, Data Curation, Visualization, Writing—review and editing; J.K.—Writing—review and editing, Supervision. All authors have read and agreed to the published version of the manuscript.

Funding: This research received no external funding.

Institutional Review Board Statement: This article contains no studies with human or animal subjects conducted by any of the authors.

Informed Consent Statement: Not applicable.

Data Availability Statement: Data sharing is not applicable to this article.

Conflicts of Interest: The authors declare no conflict of interest.

References

1. Guo, Y.R.; Cao, Q.D.; Hong, Z.S.; Tan, Y.Y.; Chen, S.D.; Jin, H.J.; Tan, K.S.; Wang, D.Y.; Yan, Y. The origin, transmission and clinical therapies on coronavirus disease 2019 (COVID-19) outbreak—an update on the status. *Mil. Med. Res.* **2020**, *7*, 1–10. [CrossRef] [PubMed]
2. Lu, R.; Zhao, X.; Li, J.; Niu, P.; Yang, B.; Wu, H.; Wang, W.; Song, H.; Huang, B.; Zhu, N.; et al. Genomic characterisation and epidemiology of 2019 novel coronavirus: Implications for virus origins and receptor binding. *Lancet* **2020**, *395*, 565–574. [CrossRef] [PubMed]
3. Dansana, D.; Kumar, R.; Bhattacharjee, A.; Hemanth, D.J.; Gupta, D.; Khanna, A.; Castillo, O. Early diagnosis of COVID-19-affected patients based on X-ray and computed tomography images using deep learning algorithm. *Soft Comput.* **2020**, *27*, 2635–2643. [CrossRef]
4. WHO. Coronavirus Disease (COVID-2019) Situation Reports. Available online: <https://www.who.int/emergencies/diseases/novel-coronavirus-2019/situationreports> (accessed on 22 July 2020).
5. Chan-Yeung, M.; Xu, R.H. SARS: Epidemiology. *Respirology* **2003**, *8*, S9–S14. [CrossRef] [PubMed]
6. Zaki, A.M.; Van Boheemen, S.; Bestebroer, T.M.; Osterhaus, A.D.M.E.; Fouchier, R.A.M. Isolation of a Novel Coronavirus from a Man with Pneumonia in Saudi Arabia. *N. Engl. J. Med.* **2012**, *367*, 1814–1820. [CrossRef] [PubMed]
7. Lee, J.; Chowell, G.; Jung, E. A dynamic compartmental model for the Middle East respiratory syndrome outbreak in the Republic of Korea: A retrospective analysis on control interventions and superspreading events. *J. Theor. Biol.* **2016**, *408*, 118–126. [CrossRef]
8. Bharati, S.; Podder, P.; Mondal, M.R.; Podder, P.; Kose, U. A review on epidemiology, genomic characteristics, spread, and treatments of COVID-19. In *Data Science for COVID-19*; Elsevier: Amsterdam, The Netherlands, 2022; pp. 487–505.
9. Chan, J.F.; Yuan, S.; Kok, K.H.; To, K.K.; Chu, H.; Yang, J.; Xing, F.; Liu, J.; Yip, C.C.; Poon, R.W.; et al. A familial cluster of pneumonia associated with the 2019 novel coronavirus indicating person-to-person transmission: A study of a family cluster. *Lancet* **2020**, *395*, 514–523. [CrossRef]
10. Podder, P.; Khamparia, A.; Mondal, M.R.; Rahman, M.A.; Bharati, S. Forecasting the Spread of COVID-19 and ICU Requirements. *Int. J. Online Biomed. Eng.* **2021**, *17*, 5. [CrossRef]
11. Mondal, M.R.; Bharati, S.; Podder, P.; Podder, P. Data analytics for novel coronavirus disease. *Inform. Med. Unlocked vol.* **2020**, *20*, 100374. [CrossRef]
12. Khanam, F.; Nowrin, I.; Mondal, M.R.H. Data Visualization and Analyzation of COVID-19. *J. Sci. Res. Rep.* **2020**, 42–52. [CrossRef]
13. Zhang, X.; Ruan, Z.; Zheng, M.; Barzel, B.; Boccaletti, S. Epidemic spreading under infection-reduced-recovery. *Chaos Solitons Fractals* **2020**, *140*, 110130. [CrossRef]
14. Brezulianu, A.; Geman, O.; Arif, M.; Chiuchisan, I.; Postolache, O.; Wang, G. Epidemiologic Evolution Platform Using Integrated Modeling and Geographic Information System. *Comput. Mater. Contin.* **2021**, *67*, 1645–1663. [CrossRef]
15. Abdulkareem, K.H.; Mohammed, M.A.; Salim, A.; Arif, M.; Geman, O.; Gupta, D.; Khanna, A. Realizing an Effective COVID-19 Diagnosis System Based on Machine Learning and IoT in Smart Hospital Environment. *IEEE Internet Things J.* **2021**, *8*, 15919–15928. [CrossRef]
16. Dourado, C.M.; da Silva, S.P.; da Nobrega, R.V.; Reboucas Filho, P.P.; Muhammad, K.; de Albuquerque, V.H. An open IoHT-based deep learning framework for online medical image recognition. *IEEE J. Sel. Areas Commun.* **2020**, *39*, 541–548. [CrossRef]
17. Egala, B.S.; Pradhan, A.K.; Badarla, V.; Mohanty, S.P. Fortified-Chain: A Blockchain-Based Framework for Security and Privacy-Assured Internet of Medical Things With Effective Access Control. *IEEE Internet Things J.* **2021**, *8*, 11717–11731. [CrossRef]
18. Podder, P.; Bharati, S.; Mondal, M.R.H.; Kose, U. 9—Application of machine learning for the diagnosis of COVID-19. In *Data Science for COVID-19*; Academic Press: Cambridge, MA, USA, 2021; pp. 175–194. [CrossRef]
19. Bharati, S.; Podder, P.; Mondal, M.; Prasath, V.B. Medical Imaging with Deep Learning for COVID-19 Diagnosis: A Comprehensive Review. *Int. J. Comput. Inf. Syst. Ind. Manag. Appl.* **2021**, *13*, 91–112.
20. Wang, L.; Wang, Y.; Ye, D.; Liu, Q. A review of the 2019 Novel Coronavirus (COVID-19) based on current evidence. *Int. J. Antimicrob. Agents* **2020**, *55*, 105948. [CrossRef]
21. Pham, Q.-V.; Nguyen, D.C.; Huynh-The, T.; Hwang, W.-J.; Pathirana, P.N. Artificial Intelligence (AI) and Big Data for Coronavirus (COVID-19) Pandemic: A Survey on the State-of-the-Arts. *IEEE Access* **2020**, *8*, 130820–130839. [CrossRef]
22. Jamshidi, M.B.; Lalbakhsh, A.; Talla, J.; Peroutka, Z.; Hadjilooei, F.; Lalbakhsh, P.; Jamshidi, M.; La Spada, L.; Mirmozafari, M.; Dehghani, M.; et al. Artificial Intelligence and COVID-19: Deep Learning Approaches for Diagnosis and Treatment. *IEEE Access* **2020**, *8*, 109581–109595. [CrossRef]
23. Nola, A.D.; Vitale, G. Łukasiewicz logic and artificial neural networks. In *Beyond Traditional Probabilistic Data Processing Techniques: Interval, Fuzzy, etc. Methods and Their Applications*; Springer: New York, NY, USA, 2020; pp. 137–149.
24. Das Chagas, J.V.S.; Rodrigues, D.d.A.; Ivo, R.F.; Hassan, M.M.; de Albuquerque, V.H.C.; Filho, P.P.R. A new approach for the detection of pneumonia in children using CXR images based on an real-time IoT system. *J. Real-Time Image Process.* **2021**, *18*, 1099–1114. [CrossRef]
25. Ohata, E.F.; das Chagas, J.V.S.; Bezerra, G.M.; Hassan, M.M.; de Albuquerque, V.H.C.; Filho, P.P.R. A novel transfer learning approach for the classification of histological images of colorectal cancer. *J. Supercomput.* **2021**, *77*, 9494–9519. [CrossRef]
26. Marques, J.A.; Han, T.; Wu, W.; do Vale Madeiro, J.P.; Neto, A.V.; Gravina, R.; Fortino, G.; de Albuquerque, V.H. IoT-based Smart Health System for Ambulatory Maternal and Fetal Monitoring. *IEEE Internet Things J.* **2020**, *8*, 16814–16824. [CrossRef]

27. Swapnarekha, H.; Behera, H.S.; Nayak, J.; Naik, B. Role of Intelligent Computing in COVID-19 Prognosis: A State-of-the-Art Review. *Chaos Solitons Fractals* **2020**, *138*, 109947. [CrossRef] [PubMed]
28. Sufian, A.; Ghosh, A.; Sadiq, A.S.; Smarandache, F. A Survey on Deep Transfer Learning to Edge Computing for Mitigating the COVID-19 Pandemic. *J. Syst. Arch.* **2020**, *108*, 101830. [CrossRef]
29. Monshi, M.M.A.; Poon, J.; Chung, V. Deep learning in generating radiology reports: A survey. *Artif. Intell. Med.* **2020**, *106*, 101878. [CrossRef]
30. Goodfellow, I.; Bengio, Y.; Courville, A. *Deep Learning*; MIT Press: Cambridge, UK, 2016.
31. LeCun, Y.; Bengio, Y.; Hinton, G. Deep learning. *Nature* **2015**, *521*, 436–444. [CrossRef]
32. Shin, H.C.; Roth, H.R.; Gao, M.; Lu, L.; Xu, Z.; Nogues, I.; Yao, J.; Mollura, D.; Summers, R.M. Deep convolutional neural networks for computer-aided detection: CNN architectures, dataset characteristics and transfer learning. *IEEE Trans. Med. Imaging* **2016**, *35*, 1285–1298. [CrossRef]
33. Litjens, G.; Kooi, T.; Bejnordi, B.E.; Setio, A.A.A.; Ciompi, F.; Ghafoorian, M.; van der Laak, J.A.W.M.; van Ginneken, B.; Sánchez, C.I. A survey on deep learning in medical image analysis. *Med. Image Anal.* **2017**, *42*, 60–88. [CrossRef]
34. Das, S. CNN Architectures: LeNet, AlexNet, VGG, GoogLeNet, ResNet and More. Available online: <https://medium.com/analytics-vidhya/cnns-architectures-lexnet-alexnet-vgg-googlenet-resnet-and-more-666091488df5> (accessed on 18 December 2020).
35. Mondal, M.R.H.; Bharati, S.; Podder, P. Diagnosis of COVID-19 Using Machine Learning and Deep Learning: A Review. *Curr. Med. Imaging Former. Curr. Med. Imaging Rev.* **2021**, *17*, 1403–1418. [CrossRef]
36. Mooney, P. Chest X-ray Images (Pneumonia). Kaggle Repository. Available online: <https://www.kaggle.com/paultimothymooney/chest-xray-pneumonia> (accessed on 1 June 2023).
37. Cohen, J.P.; Morrison, P.; Dao, L.; Roth, K.; Duong, T.; Ghassem, M. COVID-19 Image Data Collection: Prospective Predictions are the Future. *J. Mach. Learn. Biomed. Imaging* **2020**, *1*, 1–38. [CrossRef]
38. Open Database of COVID-19 Cases with Chest X-ray or CT Images. Available online: <https://github.com/ieee8023/covid-chestxray-dataset> (accessed on 1 June 2023).
39. COVIDx Dataset. Available online: <https://github.com/lindawangg/COVID-Net> (accessed on 1 June 2023).
40. COVNet. Available online: <https://github.com/bkong999/COVNet> (accessed on 7 March 2020).
41. Loey, M.; Smarandache, F.; Khalifa, N.E.M. Within the Lack of Chest COVID-19 X-ray Dataset: A Novel Detection Model Based on GAN and Deep Transfer Learning. *Symmetry* **2020**, *12*, 651. [CrossRef]
42. Loey, M. Dataset. Available online: <https://drive.google.com/uc?id=1coM7x3378f-Ou2l6Pg2wldaOI7Dntu1a> (accessed on 5 April 2020).
43. Ahmed, A. Pneumonia Sample X-rays. Available online: <https://www.kaggle.com/ahmedali2019/pneumonia-sample-xrays> (accessed on 10 March 2020).
44. Rahman, M.C.T.; Khandakar, A. COVID-19 Radiography Database. Available online: <https://www.kaggle.com/tawsifurrahman/covid19-radiography-database/data> (accessed on 1 June 2023).
45. Praveen. CoronaHack: Chest X-Ray-Dataset. Available online: <https://www.kaggle.com/praveengovi/coronahack-chest-xraydataset> (accessed on 1 June 2023).
46. TWITTER COVID-19 CXR. Available online: <https://twitter.com/ChestImaging> (accessed on 25 June 2023).
47. Covid19 Radiography Database. Available online: <https://www.kaggle.com/tawsifurrahman/covid19-radiography-databaseradiography-database> (accessed on 1 June 2023).
48. Somai, S.-I. COVID-19 Database. 2020. Available online: <https://www.sirm.org/category/senza-categoria/covid-19/> (accessed on 1 June 2023).
49. Radiopedia. Available online: <https://radiopaedia.org/search?lang=us&page=4&q=covid+19&scope=all&utf8=%E2%9C%93> (accessed on 20 June 2023).
50. Imaging, C. This Is a Thread of COVID-19 CXR (all SARS-CoV-2 PCR+) from my Hospital (Spain). I Hope It Could Help. 2020. Available online: <https://threadreaderapp.com/thread/1243928581983670272.html> (accessed on 10 June 2023).
51. COVID-19 CT Segmentation Datasets. Available online: <http://medicalsegmentation.com/covid19/> (accessed on 21 June 2023).
52. Ma, J. COVID-19-CT-Seg-Benchmark. Available online: <https://gitee.com/junma11/COVID-19-CT-Seg-Benchmark> (accessed on 31 July 2020).
53. COVID-19-TweetIDs. Available online: <https://github.com/echen102/COVID-19-TweetIDs> (accessed on 31 July 2020).
54. Coronacases Initiative. Available online: <https://coronacases.org> (accessed on 31 July 2020).
55. Mondal, M.R.H.; Bharati, S.; Podder, P. CO-IRv2: Optimized InceptionResNetV2 for COVID-19 detection from chest CT images. *PLoS ONE* **2021**, *16*, e0259179. [CrossRef]
56. Bharati, S.; Podder, P.; Mondal, M.R. *X-Ray Images Three Levels*; Figshare: Pittsburgh, PA, USA, 2021; Available online: https://figshare.com/articles/dataset/X-ray_images_three_levels/14755965/1 (accessed on 12 January 2023).
57. Kermany, D.S.; Goldbaum, M.; Cai, W.; Valentim, C.C.S.; Liang, H.; Baxter, S.L.; McKeown, A.; Yang, G.; Wu, X.; Yan, F.; et al. Identifying Medical Diagnoses and Treatable Diseases by Image-Based Deep Learning. *Cell* **2018**, *172*, 1122–1131.e9. [CrossRef]
58. Hosseiny, M.; Kooraki, S.; Gholamrezaezhad, A.; Reddy, S.; Myers, L. Radiology Perspective of Coronavirus Disease 2019 (COVID-19): Lessons From Severe Acute Respiratory Syndrome and Middle East Respiratory Syndrome. *Am. J. Roentgenol.* **2020**, *214*, 1078–1082. [CrossRef]

59. Chen, E.; Lerman, K.; Ferrara, E. COVID-19: The first public coronavirus twitter dataset. *arXiv* **2020**, arXiv:2003.07372.
60. R.S.O.N. America. RSNA Pneumonia Detection Challenge. Available online: <https://www.kaggle.com/c/rsnapneumonia-detection-challenge/data> (accessed on 1 June 2023).
61. Jun, M.; Cheng, G.; Yixin, W.; Xingle, A.; Jiantao, G.; Ziqi, Y.; Mingqing, Z.; Xin, L.; Xueyuan, D.; Shucheng, C. COVID-19 CT Lung and Infection Segmentation Dataset. *Zenodo* **2020**, *20*. Available online: <https://zenodo.org/record/3757476> (accessed on 28 June 2023).
62. Narin, A.; Kaya, C.; Pamuk, Z. Automatic detection of coronavirus disease (COVID-19) using X-ray images and deep convolutional neural networks. *Pattern Anal. Appl.* **2021**, *24*, 1207–1220. [[CrossRef](#)] [[PubMed](#)]
63. Wang, L.; Lin, Z.Q.; Wong, A. COVID-Net: A tailored deep convolutional neural network design for detection of COVID-19 cases from chest X-ray images. *Sci. Rep.* **2020**, *10*, 19549. [[CrossRef](#)] [[PubMed](#)]
64. Ghoshal, B.; Tucker, A. Estimating uncertainty and interpretability in deep learning for coronavirus (COVID-19) detection. *arXiv* **2020**, arXiv:2003.10769.
65. Zhang, J.; Xie, Y.; Pang, G.; Liao, Z.; Verjans, J.; Li, W.; Sun, Z.; He, J.; Li, Y.; Shen, C. COVID-19 screening on chest x-ray images using deep learning based anomaly detection. *arXiv* **2020**, arXiv:2003.12338.
66. Ozturk, T.; Talo, M.; Yildirim, E.A.; Baloglu, U.B.; Yildirim, O.; Acharya, U.R. Automated detection of COVID-19 cases using deep neural networks with X-ray images. *Comput. Biol. Med.* **2020**, *121*, 103792. [[CrossRef](#)]
67. Kermany, D.; Zhang, K.; Goldbaum, M. Labeled optical coherence tomography (OCT) and Chest X-Ray images for classification. *Mendeley Data Vol.* **2018**, *2*, 651.
68. Mahmud, T.; Rahman, A.; Fattah, S.A. CovXNet: A multi-dilation convolutional neural network for automatic COVID-19 and other pneumonia detection from chest X-ray images with transferable multi-receptive feature optimization. *Comput. Biol. Med.* **2020**, *122*, 103869. [[CrossRef](#)]
69. Chest X-Ray Images (Pneumonia). Available online: <https://www.kaggle.com/paultimothymooney/chestxray-pneumonia> (accessed on 22 July 2020).
70. Khan, A.I.; Shah, J.L.; Bhat, M.M. CoroNet: A deep neural network for detection and diagnosis of COVID-19 from chest x-ray images. *Comput. Methods Programs Biomed.* **2020**, *196*, 105581. [[CrossRef](#)]
71. Toğaçar, M.; Ergen, B.; Cömert, Z. COVID-19 detection using deep learning models to exploit Social Mimic Optimization and structured chest X-ray images using fuzzy color and stacking approaches. *Comput. Biol. Med.* **2020**, *121*, 103805. [[CrossRef](#)]
72. Ucar, F.; Korkmaz, D. COVIDiagnosis-Net: Deep Bayes-SqueezeNet based Diagnostic of the Coronavirus Disease 2019 (COVID-19) from X-Ray Images. *Med. Hypotheses* **2020**, *140*, 109761. [[CrossRef](#)]
73. Wang, X.; Peng, Y.; Lu, L.; Lu, Z.; Bagheri, M.; Summers, R.M. Chestx-ray8: Hospital-scale chest x-ray database and benchmarks on weakly-supervised classification and localization of common thorax diseases. *arXiv* **2017**, arXiv:1705.02315. [[CrossRef](#)]
74. Chowdhury, M.E.H.; Rahman, T.; Khandakar, A.; Mazhar, R.; Kadir, M.A.; Bin Mahbub, Z.; Islam, K.R.; Khan, M.S.; Iqbal, A.; Al Emadi, N.; et al. Can AI Help in Screening Viral and COVID-19 Pneumonia? *IEEE Access* **2020**, *8*, 132665–132676. [[CrossRef](#)]
75. Zheng, C.; Deng, X.; Fu, Q.; Zhou, Q.; Feng, J.; Ma, H.; Liu, W.; Wang, X. Deep learning-based detection for COVID-19 from chest CT using weak label. *medRxiv* **2020**. [[CrossRef](#)]
76. Chen, J.; Wu, L.; Zhang, J.; Zhang, L.; Gong, D.; Zhao, Y.; Chen, Q.; Huang, S.; Yang, M.; Yang, X. Deep learning-based model for detecting 2019 novel coronavirus pneumonia on high-resolution computed tomography: A prospective study. *medRxiv* **2020**, *18*, 19196. [[CrossRef](#)]
77. Jin, S.; Wang, B.; Xu, H.; Luo, C.; Wei, L.; Zhao, W.; Hou, X.; Ma, W.; Xu, Z.; Zheng, Z. AI-assisted CT imaging analysis for COVID-19 screening: Building and deploying a medical AI system in four weeks. *medRxiv* **2020**. [[CrossRef](#)]
78. Jin, S.; Wang, B.; Xu, H.; Luo, C.; Wei, L.; Zhao, W.; Hou, X.; Ma, W.; Xu, Z.; Zheng, Z. Artificial intelligence distinguishes COVID-19 from community acquired pneumonia on chest CT. *Radiology* **2020**, *23*, 200905.
79. Song, Y.; Zheng, S.; Li, L.; Zhang, X.; Zhang, X.; Huang, Z.; Chen, J.; Zhao, H.; Jie, Y.; Wang, R. Deep learning Enables Accurate Diagnosis of Novel Coronavirus (COVID-19) with CT images. *medRxiv* **2020**. [[CrossRef](#)] [[PubMed](#)]
80. Long, C.; Xu, H.; Shen, Q.; Zhang, X.; Fan, B.; Wang, C.; Zeng, B.; Li, Z.; Li, X.; Li, H. Diagnosis of the Coronavirus disease (COVID-19): rRT-PCR or CT? *Eur. J. Radiol.* **2020**, *126*, 108961. [[CrossRef](#)] [[PubMed](#)]
81. Bernheim, A.; Mei, X.; Huang, M.; Yang, Y.; Fayad, Z.A.; Zhang, N.; Diao, K.; Lin, B.; Zhu, X.; Li, K.; et al. Chest CT Findings in Coronavirus Disease-19 (COVID-19): Relationship to Duration of Infection. *Radiology* **2020**, *295*, 200463. [[CrossRef](#)]
82. Ardakani, A.A.; Kanafi, A.R.; Acharya, U.R.; Khadem, N.; Mohammadi, A. Application of deep learning technique to manage COVID-19 in routine clinical practice using CT images: Results of 10 convolutional neural networks. *Comput. Biol. Med.* **2020**, *121*, 103795. [[CrossRef](#)]
83. Yang, X.; He, X.; Zhao, J.; Zhang, Y.; Zhang, S.; Xie, P. COVID-CT-Dataset: A CT Scan Dataset about COVID-19. *arXiv* **2020**, arXiv:2003.13865.
84. Wang, L.L.; Lo, K.; Chandrasekhar, Y.; Reas, R.; Yang, J.; Burdick, D.; Eide, D.; Funk, K.; Katsis, Y.; Kinney, R.; et al. COVID-19: The COVID-19 Open Research Dataset. 2020. Available online: <https://allenai.org/data/cord-19> (accessed on 12 January 2023).
85. Acar, E.; Şahin, E.; Yılmaz, İ. Improving effectiveness of different deep learning-based models for detecting COVID-19 from computed tomography (CT) images. *medRxiv* **2020**, *33*, 17589–17609. [[CrossRef](#)]
86. Chung, N. COVID-19 Chest X-ray Data Initiative. Available online: <https://github.com/agchung/Figure1-COVID-chestxraydataset> (accessed on 12 June 2023).

87. Waheed, A.; Goyal, M.; Gupta, D.; Khanna, A.; Al-Turjman, F.; Pinheiro, P.R. CovidGAN: Data Augmentation Using Auxiliary Classifier GAN for Improved COVID-19 Detection. *IEEE Access* **2020**, *8*, 91916–91923. [[CrossRef](#)] [[PubMed](#)]
88. Hu, S.; Gao, Y.; Niu, Z.; Jiang, Y.; Li, L.; Xiao, X.; Wang, M.; Fang, E.F.; Menpes-Smith, W.; Xia, J.; et al. Weakly Supervised Deep Learning for COVID-19 Infection Detection and Classification From CT Images. *IEEE Access* **2020**, *8*, 118869–118883. [[CrossRef](#)]
89. Han, Z.; Wei, B.; Hong, Y.; Li, T.; Cong, J.; Zhu, X.; Wei, H.; Zhang, W. Accurate Screening of COVID-19 Using Attention-Based Deep 3D Multiple Instance Learning. *IEEE Trans. Med. Imaging* **2020**, *39*, 2584–2594. [[CrossRef](#)] [[PubMed](#)]
90. Roy, S.; Menapace, W.; Oei, S.; Luijten, B.; Fini, E.; Saltori, C.; Huijben, I.; Chennakeshava, N.; Mento, F.; Sentelli, A.; et al. Deep Learning for Classification and Localization of COVID-19 Markers in Point-of-Care Lung Ultrasound. *IEEE Trans. Med. Imaging* **2020**, *39*, 2676–2687. [[CrossRef](#)]
91. SKassania, S.H.; Kassanib, P.H.; Wesolowskic, M.J.; Schneidera, K.A.; Detersa, R. Automatic Detection of Coronavirus Disease (COVID-19) in X-ray and CT Images: A Machine Learning-Based Approach. *arXiv* **2020**, arXiv:2004.10641.
92. Abbas, A.; Abdelsamea, M.M.; Gaber, M.M. Classification of COVID-19 in chest X-ray images using DeTraC deep convolutional neural network. *Appl. Intell.* **2020**, *51*, 854–864. [[CrossRef](#)]
93. Khalifa, N.E.M.; Taha, M.H.N.; Hassanien, A.E.; Elghamrawy, S. Detection of Coronavirus (COVID-19) Associated Pneumonia Based on Generative Adversarial Networks and a Fine-Tuned Deep Transfer Learning Model Using Chest X-ray Dataset. *arXiv* **2020**, arXiv:2004.01184.
94. Rahimzadeh, M.; Attar, A. A New Modified Deep Convolutional Neural Network for Detecting COVID-19 from X-ray Images. *arXiv* **2020**, arXiv:2004.08052.
95. Ramadhan, M.M.; Faza, A.; Lubis, L.E.; Yunus, R.E.; Salamah, T.; Handayani, D.; Lestariningsih, I.; Resa, A.; Alam, C.R.; Prajitno, P. Fast and accurate detection of COVID-19-related pneumonia from chest X-ray images with novel deep learning model. *arXiv* **2020**, arXiv:2005.04562.
96. Khobahi, S.; Agarwal, C.; Soltanalian, M. CoroNet: A Deep Network Architecture for Semi-Supervised Task-Based Identification of COVID-19 from Chest X-ray Images. *medRxiv* **2020**, *17*, 2020–2024. [[CrossRef](#)]
97. Li, C.; Yang, Y.; Liang, H.; Wu, B. Transfer learning for establishment of recognition of COVID-19 on CT imaging using small-sized training datasets. *Knowledge-Based Syst.* **2021**, *218*, 106849. [[CrossRef](#)]
98. Gao, K.; Su, J.; Jiang, Z.; Zeng, L.-L.; Feng, Z.; Shen, H.; Rong, P.; Xu, X.; Qin, J.; Yang, Y.; et al. Dual-branch combination network (DCN): Towards accurate diagnosis and lesion segmentation of COVID-19 using CT images. *Med. Image Anal.* **2020**, *67*, 101836. [[CrossRef](#)]
99. Alshazly, H.; Linse, C.; Barth, E.; Martinetz, T. Explainable COVID-19 Detection Using Chest CT Scans and Deep Learning. *Sensors* **2021**, *21*, 455. [[CrossRef](#)]
100. Butt, C.; Gill, J.; Chun, D.; Babu, B.A. Deep learning system to screen coronavirus disease 2019 pneumonia. *Appl. Intell.* **2020**, *53*, 4874. [[CrossRef](#)]
101. Farooq, M.; Hafeez, A. COVID-resnet: A deep learning framework for screening of COVID-19 from radiographs. *arXiv* **2020**, arXiv:2003.14395.
102. Wu, X.; Hui, H.; Niu, M.; Li, L.; Wang, L.; He, B.; Yang, X.; Li, L.; Li, H.; Tian, J.; et al. Deep learning-based multi-view fusion model for screening 2019 novel coronavirus pneumonia: A multicentre study. *Eur. J. Radiol.* **2020**, *128*, 109041. [[CrossRef](#)]
103. Ouyang, X.; Huo, J.; Xia, L.; Shan, F.; Liu, J.; Mo, Z.; Yan, F.; Ding, Z.; Yang, Q.; Song, B.; et al. Dual-Sampling Attention Network for Diagnosis of COVID-19 From Community Acquired Pneumonia. *IEEE Trans. Med. Imaging* **2020**, *39*, 2595–2605. [[CrossRef](#)] [[PubMed](#)]
104. Sethy, P.K.; Behera, S.K. Detection of coronavirus disease (COVID-19) based on deep features. *Preprints* **2020**, 2020030300, 2020.
105. El Asnaoui, K.; Chawki, Y. Using X-ray images and deep learning for automated detection of coronavirus disease. *J. Biomol. Struct. Dyn.* **2020**, *39*, 3615–3626. [[CrossRef](#)] [[PubMed](#)]
106. Hall, L.O.; Paul, R.; Goldgof, D.B.; Goldgof, G.M. Finding COVID-19 from chest x-rays using deep learning on a small dataset. *arXiv* **2020**, arXiv:2004.02060.
107. Loey, M.; Manogaran, G.; Khalifa, N.E.M. A deep transfer learning model with classical data augmentation and CGAN to detect COVID-19 from chest CT radiography digital images. *Neural Comput. Appl.* **2020**, 1–13. [[CrossRef](#)]
108. Rahimzadeh, M.; Attar, A. A modified deep convolutional neural network for detecting COVID-19 and pneumonia from chest X-ray images based on the concatenation of Xception and ResNet50V2. *Inform. Med. Unlocked* **2020**, *19*, 100360. [[CrossRef](#)]
109. Bansal, N.; Sridhar, S. Classification of X-ray Images For Detecting COVID-19 Using Deep Transfer Learning. *Res. Sq.* **2020**. [[CrossRef](#)]
110. Vaid, S.; Kalantar, R.; Bhandari, M. Deep learning COVID-19 detection bias: Accuracy through artificial intelligence. *Int. Orthop.* **2020**, *44*, 1539–1542. [[CrossRef](#)]
111. Yang, K.; Liu, X.; Yang, Y.; Liao, X.; Wang, R.; Zeng, X.; Wang, Y.; Zhang, M.; Zhang, T. End-to-end COVID-19 screening with 3D deep learning on chest computed tomography. *Res. Sq.* **2020**. [[CrossRef](#)]
112. Panwar, H.; Gupta, P.; Siddiqui, M.K.; Morales-Menendez, R.; Singh, V. Application of deep learning for fast detection of COVID-19 in X-Rays using nCOVnet. *Chaos Solitons Fractals* **2020**, *138*, 109944. [[CrossRef](#)]
113. Brunese, L.; Mercaldo, F.; Reginelli, A.; Santone, A. Explainable Deep Learning for Pulmonary Disease and Coronavirus COVID-19 Detection from X-rays. *Comput. Methods Programs Biomed.* **2020**, *196*, 105608. [[CrossRef](#)] [[PubMed](#)]

114. Saeedi, A.; Saeedi, M.; Maghsoudi, A. A novel and reliable deep learning web-based tool to detect COVID-19 infection form chest CT-scan. *arXiv* **2020**, arXiv:2006.14419.
115. Bassi, P.R.A.S.; Attux, R. A deep convolutional neural network for COVID-19 detection using chest X-rays. *Res. Biomed. Eng.* **2021**, *38*, 139–148. [[CrossRef](#)]
116. Siddhartha, M.; Santra, A. COVIDLite: A depth-wise separable deep neural network with white balance and CLAHE for detection of COVID-19. *arXiv* **2020**, arXiv:2006.13873.
117. Bharati, S.; Podder, P.; Mondal, M.R.H.; Prasath, V.S. CO-ResNet: Optimized ResNet model for COVID-19 diagnosis from X-ray images. *Int. J. Hybrid Intell. Syst.* **2021**, *17*, 71–85. [[CrossRef](#)]
118. Nassif, A.B.; Shahin, I.; Bader, M.; Hassan, A.; Werghe, N. COVID-19 Detection Systems Using Deep-Learning Algorithms Based on Speech and Image Data. *Mathematics* **2022**, *10*, 564. [[CrossRef](#)]
119. Chakraborty, S.; Murali, B.; Mitra, A.K. An Efficient Deep Learning Model to Detect COVID-19 Using Chest X-ray Images. *Int. J. Environ. Res. Public Health* **2022**, *19*, 2013. [[CrossRef](#)]
120. Bharati, S.; Podder, P.; Mondal, M.R.H.; Gandhi, N. Optimized NASNet for Diagnosis of COVID-19 from Lung CT Images. In Proceedings of the 20th International Conference on Intelligent Systems Design and Applications (ISDA 2020), Online, 12–15 December 2020.
121. Raihan-Al-Masud, M.; Mondal, M.R. Data-driven diagnosis of spinal abnormalities using feature selection and machine learning algorithms. *PLoS ONE* **2020**, *15*, e0228422. [[CrossRef](#)]
122. Bharati, S.; Podder, P.; Mondal, R.; Mahmood, A.; Masud, R.A. Comparative Performance Analysis of Different Classification Algorithm for the Purpose of Prediction of Lung Cancer. In *Intelligent Systems Design and Applications. ISDA 2018 2018. Advances in Intelligent Systems and Computing*; Abraham, A., Cherukuri, A., Melin, P., Gandhi, N., Eds.; Springer: Cham, Switzerland, 2019; Volume 941, pp. 447–457. [[CrossRef](#)]
123. Bharati, S.; Rahman, M.A.; Podder, P. Breast Cancer Prediction Applying Different Classification Algorithm with Comparative Analysis using WEKA. In Proceedings of the 2018 4th International Conference on Electrical Engineering and Information & Communication Technology (iCEEICT), Dhaka, Bangladesh, 13–15 September 2018; pp. 581–584. [[CrossRef](#)]
124. Bharati, S.; Podder, P.; Mondal, M.R.H. Hybrid deep learning for detecting lung diseases from X-ray images. *Inform. Med. Unlocked* **2020**, *20*, 100391. [[CrossRef](#)] [[PubMed](#)]
125. Zhou, T.; Lu, H.; Yang, Z.; Qiu, S.; Huo, B.; Dong, Y. The ensemble deep learning model for novel COVID-19 on CT images. *Appl. Soft Comput.* **2021**, *98*, 106885. [[CrossRef](#)] [[PubMed](#)]
126. Rehman, A.; Naz, S.; Khan, A.; Zaib, A.; Razzak, I. Improving Coronavirus (COVID-19) Diagnosis Using Deep Transfer Learning. In *Proceedings of International Conference on Information Technology and Applications*; Ullah, A., Anwar, S., Rocha, Á., Gill, S., Eds.; Lecture Notes in Networks and Systems; Springer: Singapore, 2022; Volume 350, pp. 23–37. [[CrossRef](#)]
127. Xu, X.; Jiang, X.; Ma, C.; Du, P.; Li, X.; Lv, S.; Yu, L.; Chen, Y.; Su, J.; Lang, G. Deep Learning System to Screen novel Coronavirus Disease 2019 Pneumonia. *Engineering* **2020**, *6*, 1122–1129. [[CrossRef](#)]
128. Wang, S.; Kang, B.; Ma, J.; Zeng, X.; Xiao, M.; Guo, J.; Cai, M.; Yang, J.; Li, Y.; Meng, X.; et al. A deep learning algorithm using CT images to screen for Corona Virus Disease (COVID-19). *Eur. Radiol.* **2020**, *31*, 6096–6104. [[CrossRef](#)] [[PubMed](#)]
129. Turkoglu, M. COVID-19 Detection System Using Chest CT Images and Multiple Kernels-Extreme Learning Machine Based on Deep Neural Network. *IRBM* **2021**, *42*, 207–214. [[CrossRef](#)] [[PubMed](#)]
130. Ohata, E.F.; Bezerra, G.M.; das Chagas, J.V.S.; Neto, A.V.L.; Albuquerque, A.B.; de Albuquerque, V.H.C.; Filho, P.P.R. Automatic detection of COVID-19 infection using chest X-ray images through transfer learning. *IEEE/CAA J. Autom. Sin.* **2020**, *8*, 239–248. [[CrossRef](#)]
131. Hussain, E.; Hasan, M.; Rahman, A.; Lee, I.; Tamanna, T.; Parvez, M.Z. CoroDet: A deep learning based classification for COVID-19 detection using chest X-ray images. *Chaos Solitons Fractals* **2020**, *142*, 110495. [[CrossRef](#)]
132. Bhattacharyya, A.; Bhaik, D.; Kumar, S.; Thakur, P.; Sharma, R.; Pachori, R.B. A deep learning based approach for automatic detection of COVID-19 cases using chest X-ray images. *Biomed. Signal Process. Control.* **2022**, *71*, 103182. [[CrossRef](#)]
133. Kumar, R.; Khan, A.A.; Kumar, J.; Zakria, A.; Golilarz, N.A.; Zhang, S.; Ting, Y.; Zheng, C.; Wang, W. Blockchain-Federated-Learning and Deep Learning Models for COVID-19 Detection Using CT Imaging. *IEEE Sens. J.* **2021**, *21*, 16301–16314. [[CrossRef](#)]
134. Yan, B.; Wang, J.; Cheng, J.; Zhou, Y.; Zhang, Y.; Yang, Y.; Liu, L.; Zhao, H.; Wang, C.; Liu, B. Experiments of Federated Learning for COVID-19 Chest X-ray Images. In *Advances in Artificial Intelligence and Security. ICAIS 2021. Communications in Computer and Information Science*; Sun, X., Zhang, X., Xia, Z., Bertino, E., Eds.; Springer: Cham, Switzerland, 2021; Volume 1423, pp. 41–53. [[CrossRef](#)]
135. Zhang, W.; Zhou, T.; Lu, Q.; Wang, X.; Zhu, C.; Sun, H.; Wang, Z.; Lo, S.K.; Wang, F.-Y. Dynamic-Fusion-Based Federated Learning for COVID-19 Detection. *IEEE Internet Things J.* **2021**, *8*, 15884–15891. [[CrossRef](#)] [[PubMed](#)]
136. Feki, I.; Ammar, S.; Kessentini, Y.; Muhammad, K. Federated learning for COVID-19 screening from Chest X-ray images. *Appl. Soft Comput.* **2021**, *106*, 107330. [[CrossRef](#)] [[PubMed](#)]
137. Dou, Q.; So, T.Y.; Jiang, M.; Liu, Q.; Vardhanabhuti, V.; Kaissis, G.; Li, Z.; Si, W.; Lee, H.H.C.; Yu, K.; et al. Federated deep learning for detecting COVID-19 lung abnormalities in CT: A privacy-preserving multinational validation study. *NPJ Digit. Med.* **2021**, *4*, 60. [[CrossRef](#)]

138. Yang, D.; Xu, Z.; Li, W.; Myronenko, A.; Roth, H.R.; Harmon, S.; Xu, S.; Turkbey, B.; Turkbey, E.; Wang, X.; et al. Federated semi-supervised learning for COVID region segmentation in chest CT using multi-national data from China, Italy, Japan. *Med. Image Anal.* **2021**, *70*, 101992. [CrossRef]
139. Sattler, F.; Müller, K.R.; Samek, W. Clustered federated learning: Model-agnostic distributed multitask optimization under privacy constraints. *IEEE Trans. Neural Netw. Learn. Syst.* **2020**, *32*, 3710–3722. [CrossRef]
140. Jiang, Y.; Konečný, J.; Rush, K.; Kannan, S. Improving federated learning personalization via model agnostic meta learning. *arXiv* **2019**, arXiv:1909.12488.
141. Corinzia, L.; Beuret, A.; Buhmann, J.M. Variational federated multi-task learning. *arXiv* **2019**, arXiv:1906.06268.
142. Kim, Y.J.; Hong, C.S. Blockchain-based Node-aware Dynamic Weighting Methods for Improving Federated Learning Performance. In Proceedings of the 20th Asia-Pacific Network Operations and Management Symposium (APNOMS), Matsue, Japan, 18–20 September 2019; pp. 1–4. [CrossRef]
143. Kim, H.; Park, J.; Bennis, M.; Kim, S.-L. Blockchained On-Device Federated Learning. *IEEE Commun. Lett.* **2019**, *24*, 1279–1283. [CrossRef]
144. Dayan, I.; Roth, H.R.; Zhong, A.; Harouni, A.; Gentili, A.; Abidin, A.Z.; Liu, A.; Costa, A.B.; Wood, B.J.; Tsai, C.-S.; et al. Federated learning for predicting clinical outcomes in patients with COVID-19. *Nat. Med.* **2021**, *27*, 1735–1743. [CrossRef]
145. Lo, S.K.; Lu, Q.; Wang, C.; Paik, H.Y.; Zhu, L. A systematic literature review on federated machine learning: From a software engineering perspective. *ACM Comput. Surv. (CSUR)* **2021**, *54*, 1–39. [CrossRef]
146. Eduardo, P. SARS-CoV-2 Ct-Scan Dataset. Available online: <https://www.kaggle.com/plameneduardo/sarscov2-ctscan-dataset> (accessed on 18 December 2020).
147. Kingma, D.P.; Ba, J. Adam: A method for stochastic optimization. *arXiv* **2014**, arXiv:1412.6980.
148. Zou, F.; Shen, L.; Jie, Z.; Zhang, W.; Liu, W. A Sufficient Condition for Convergences of Adam and RMSProp. *arXiv* **2019**, arXiv:1811.09358. [CrossRef]
149. Duchi, J.; Hazan, E.; Singer, Y. Adaptive subgradient methods for online learning and stochastic optimization. *J. Mach. Learn. Res.* **2011**, *12*, 7.
150. Shoeibi, A.; Khodatars, M.; Alizadehsani, R.; Ghassemi, N.; Jafari, M.; Moridian, P.; Khadem, A.; Sadeghi, D.; Hussain, S.; Zare, A. Automated detection and forecasting of COVID-19 using deep learning techniques: A review. *arXiv* **2020**, arXiv:2007.10785.
151. Islam, M.; Karray, F.; Alhaji, R.; Zeng, J. A Review on Deep Learning Techniques for the Diagnosis of Novel Coronavirus (COVID-19). *IEEE Access* **2021**, *9*, 30551–30572. [CrossRef] [PubMed]
152. Ghaderzadeh, M.; Asadi, F. Deep Learning in the Detection and Diagnosis of COVID-19 Using Radiology Modalities: A Systematic Review. *J. Health Eng.* **2021**, *2021*, 6677314. [CrossRef]
153. Low, W.C.S.; Chuah, J.H.; Tee, C.A.T.H.; Anis, S.; Shoaib, M.A.; Faisal, A.; Khalil, A.; Lai, K.W. An Overview of Deep Learning Techniques on Chest X-Ray and CT Scan Identification of COVID-19. *Comput. Math. Methods Med.* **2021**, *2021*, 5528144. [CrossRef]
154. Alafif, T.; Tehame, A.M.; Bajaba, S.; Barnawi, A.; Zia, S. Machine and Deep Learning towards COVID-19 Diagnosis and Treatment: Survey, Challenges, and Future Directions. *Int. J. Environ. Res. Public Health* **2021**, *18*, 1117. [CrossRef]
155. Moghaddam, J.; Mohammad, S. A novel framework based on deep learning for COVID-19 diagnosis from X-ray images. *PeerJ Comput. Sci.* **2023**, *9*, e1375.
156. Kainat, K.; Usman, M.; Fong, A. Deep learning framework for early detection of COVID-19 using X-ray images. *Multimed. Tools Appl.* **2023**, 1–26. [CrossRef]
157. AlMohimeed, A.; Saleh, H.; El-Rashidy, N.; Saad, R.M.A.; El-Sappagh, S.; Mostafa, S. Diagnosis of COVID-19 Using Chest X-ray Images and Disease Symptoms Based on Stacking Ensemble Deep Learning. *Diagnostics* **2023**, *13*, 1968. [CrossRef]
158. Al-Waisy, A.S.; Al-Fahdawi, S.; Mohammed, M.A.; Abdulkareem, K.H.; Mostafa, S.A.; Maashi, M.S.; Arif, M.; Garcia-Zapirain, B. COVID-CheXNet: Hybrid deep learning framework for identifying COVID-19 virus in chest X-rays images. *Soft Comput.* **2023**, *27*, 2657–2672. [CrossRef]
159. Kathamuthu, N.D.; Subramaniam, S.; Le, Q.H.; Muthusamy, S.; Panchal, H.; Sundararajan, S.C.; Alrubaie, A.J.; Zahra, M.M. A deep transfer learning-based convolution neural network model for COVID-19 detection using computed tomography scan images for medical applications. *Adv. Eng. Softw.* **2023**, *175*, 103317. [CrossRef]
160. Celik, G. Detection of COVID-19 and other pneumonia cases from CT and X-ray chest images using deep learning based on feature reuse residual block and depthwise dilated convolutions neural network. *Appl. Soft Comput.* **2023**, *133*, 109906. [CrossRef]
161. Choudhary, T.; Gujar, S.; Goswami, A.; Mishra, V.; Badal, T. Deep learning-based important weights-only transfer learning approach for COVID-19 CT-scan classification. *Appl. Intell.* **2023**, *53*, 7201–7215. [CrossRef] [PubMed]
162. Constantinou, M.; Exarchos, T.; Vrahatis, A.G.; Vlamos, P. COVID-19 classification on chest X-ray images using deep learning methods. *Int. J. Environ. Res. Public Health* **2023**, *20*, 2035. [CrossRef] [PubMed]
163. Mukhi, S.E.; Varshini, R.T.; Sherley, S.E. Diagnosis of COVID-19 from Multimodal Imaging Data Using Optimized Deep Learning Techniques. *SN Comput. Sci.* **2023**, *4*, 212. [CrossRef] [PubMed]
164. Hayat, A.; Baglat, P.; Mendonça, F.; Mostafa, S.S.; Morgado-Dias, F. Novel Comparative Study for the Detection of COVID-19 Using CT Scan and Chest X-ray Images. *Int. J. Environ. Res. Public Health* **2023**, *20*, 1268. [CrossRef]
165. Zhang, X.; Han, L.; Sobeih, T.; Han, L.; Dempsey, N.; Lechareas, S.; Tridente, A.; Chen, H.; White, S.; Zhang, D. CXR-Net: A Multitask Deep Learning Network for Explainable and Accurate Diagnosis of COVID-19 Pneumonia From Chest X-Ray Images. *IEEE J. Biomed. Health Inform.* **2023**, *27*, 980–991. [CrossRef]

166. Malik, H.; Naeem, A.; Naqvi, R.A.; Loh, W.-K. DMFL_Net: A Federated Learning-Based Framework for the Classification of COVID-19 from Multiple Chest Diseases Using X-rays. *Sensors* **2023**, *23*, 743. [[CrossRef](#)]
167. Mondal, M.R.H.; Bharati, S.; Podder, P. COVID-19 CT images. figshare. *Dataset* **2021**. [[CrossRef](#)]
168. Islam, A.; Rahim, T.; Masduzzaman, M.; Shin, S.Y. A Blockchain-Based Artificial Intelligence-Empowered Contagious Pandemic Situation Supervision Scheme Using Internet of Drone Things. *IEEE Wirel. Commun.* **2021**, *28*, 166–173. [[CrossRef](#)]

Disclaimer/Publisher's Note: The statements, opinions and data contained in all publications are solely those of the individual author(s) and contributor(s) and not of MDPI and/or the editor(s). MDPI and/or the editor(s) disclaim responsibility for any injury to people or property resulting from any ideas, methods, instructions or products referred to in the content.